Article

External surface modification of as-made ZSM-5 and their catalytic performance in the methanol to propylene reaction

Xuebin Zhao [a,b,c], Yang Hong [b,c], Linying Wang [b], Dong Fan [b], Nana Yan [b,c], Xiaona Liu [b,c], Peng Tian [b,#], Xinwen Guo [a,*], Zhongmin Liu [b,$]

[a] State Key Laboratory of Fine Chemicals, PSU-DUT Joint Center for Energy Research, School of Chemical Engineering, Dalian University of Technology, Dalian 116024, Liaoning, China

[b] National Engineering Laboratory for Methanol to Olefins, State Energy Low Carbon Catalysis and Engineering R&D Center, Dalian National Laboratory for Clean Energy, Collaborative Innovation Center of Chemistry for Energy Materials (iChEM), Dalian Institute of Chemical Physics, Chinese Academy of Sciences, Dalian 116023, Liaoning, China

[c] University of Chinese Academy of Sciences, Beijing 100049, China

A B S T R A C T

Post-synthetic treatment of high-silica as-made ZSM-5 with organic template in the micropores was explored to reduce/remove the external surface acid density of ZSM-5. It is found that Na_2H_2EDTA treatment can selectively remove the surface Al atoms, but generates new acid sites (likely silanol nests) on the external surface. H_3PO_4 treatment is unable to remove surface Al atoms, while small amount of P is left on the external surface, which effectively decreases the acid density. The catalytic performance of the resultant materials is evaluated in the methanol conversion reaction. H_3PO_4 treatment can effectively improve both the catalytic lifetime and the stability of propene selectivity. This occurs due to a combination of the increased tolerance to the external coke deposition and the depressed coking rate (reduced side reactions). Na_2H_2EDTA treatment only prolongs the catalytic lifetime, resulting from the improved tolerance to the external coke deposition. Under the optimized H_3PO_4 treatment condition, the resultant ZSM-5 gives a catalytic lifetime of about 1.5 times longer than the precursor. Moreover, the propene selectivity is improved, showing a slight increasing trend until the deactivation.

1. Introduction

With the depletion of oil resource, the methanol to propene (MTP) process provides an alternative route to produce propene beyond the conventional steam cracking of naphtha and fluid catalytic cracking process [1–4]. The MTP reaction has aroused significant interest in both the academic and industrial

fields since it was originally developed by Lurgi company [1]. It has been recognized that the methanol conversion over zeolite catalysts is a typical acid catalyzed process and coke deposition is the main cause of the catalyst deactivation [5–8]. ZSM-5 zeolite, with a 3D interconnected pore system composed of 10-membered rings, is currently the most effective catalyst, which has found application in the industrial fixed bed MTP

process.

Due to the space limitation in the micropores of ZSM-5 (0.51 × 0.55 nm, 0.53 × 0.56 nm), the coke deposition in the crystal interior can be greatly avoided during the MTP reaction. And the deactivation on ZSM-5 is closely related to the external surface acidity [9]. Therefore, attempts have been made to reduce the external surface acidity of ZSM-5, aiming to retard the coke deposition rate and improve the catalytic stability. The strategies developed to passivate the external surface acid sites of zeolites can be mainly classified as macromolecule deposition [10–19], synthesis of zeolites with core-shell structure [20–23], metal or non-metal modification [24–28] and so on.

The macromolecules reported for the passivation/modification of external surface acid sites of zeolites include bulky organophosphorus compounds [10,11], bulky nitrogen compounds [12] and various siloxane [14–19]. Losch et al. [29] once investigated the effect of surface passivation of nano-sized ZSM-5 on the methanol conversion reaction by a chemical liquid deposition (CLD) technique using tetraethylorthosilicate. The resultant catalyst exhibited an enhanced selectivity to lower olefins, but a significant decrease in the stability, which was due to the partial blocking of micropores (the coking process exclusively occurred within the pores and fastened the catalyst deactivation). Phosphorus modification of HZSM-5 zeolite by wet impregnation has long been known to decrease aromatic formation and improve catalytic stability in methanol conversion chemistry [26,30,31]. Impregnation of HZSM-5 with phosphoric acid leads to the hydrolysis of framework Al and the condensation of Brønsted acid sites with POH groups, resulting in higher framework Si/Al ratio and the decrease of strong acid sites [31,32]. However, phosphoric acid can deposit both in the inner pore and external surface of ZSM-5 due to its smaller size. Recently, Liu et al. [24] reported an effective method to prepare P-modified H-ZSM-5 with the preferential covering of the external surface acid sites by adding ethanol during the impregnation. This occurred because bulky organic phosphates were likely formed from the reaction of phosphoric acid and ethanol, which deposited on the external surface of HZSM-5 crystals. The obtained material gave high *p*-xylene selectivity along with a relatively high catalytic activity in toluene disproportionation reaction.

Zeolites with core-shell structure are generally synthesized by epitaxial growth of inert shell outside zeolite core. In principle, the degree of surface coverage and shell thickness are the key factors influencing the catalytic performance. Luo et al. [33] successfully synthesized ZSM-5@S-1 material, which gave comparable propene selectivity with the ZSM-5 precursor and a prolonged lifetime from 74 to 139 h in the MTP reaction. The change in lifetime should result from the reduced number of external acid sites and the attenuated occurrence of side reactions. Yin et al. [34] also demonstrated that the coverage of surface acid sites as a result of contiguous silicalite-1 coating was the reason for the high stability and selectivity of ZSM-5 in CH_3Br conversion reaction.

Recently, selective dealumination methods were reported to remove the external surface acid sites of ZSM-5. Inagaki et al. [35] found that post-synthetic HNO_3 treatment of ZSM-5 zeolite synthesized in the absence of organic structure-directing agent can selectively remove framework Al on the external surface, producing a unique ZSM-5 zeolite catalyst that has very few acid sites on its external surface. The treated ZSM-5 showed high resistance to coke formation during the cracking of hexane or other paraffin molecules.

In this contribution, a facile post-synthetic treatment method was developed to remove/modify the external surface acidity of ZSM-5 by utilizing as-made ZSM-5 containing organic structure directing agent (OSDA) as the precursor. The existence of OSDA in the as-made ZSM-5 crystals may effectively block the channels and confine the modification on the crystal exterior without altering the internal acidity and integrity of the crystals. Two common reagents, Na_2H_2EDTA and H_3PO_4, herein were explored for the post-synthetic treatment. It is mentioned that large molecule EDTA, as a powerful chelating agent, has been widely used for the dealumination of Y zeolite [36]. But its use for the dealumination of ZSM-5 is quite rare. The variations of structure integrity, surface acid density and catalytic performance of the modified ZSM-5 were investigated. Moreover, the H_3PO_4 concentration was optimized to further prolong the lifetime in the MTP reaction.

2. Experimental

2.1. Materials

The chemical reagents used in synthesis and modification of ZSM-5 zeolites include: tetraethyl orthosilicate (TEOS, Tianjin Kemiou Chemical Reagent Co), aluminium iso-propoxide (Al(OPri)$_3$, Sinopharm Chemical Reagent Co.), tetrapropylammonium hydroxide (TPAOH, 10 wt% Tianjin Jingrun Chemical Co), urea (Tianjin Damao Chemical Co), ethylenediamine tetraacetic acid disodium salt (Na$_2$H$_2$EDTA, Tianda Chemical Reagent Co. Ltd.), phosphoric acid (85.0 wt%, Sichuan Xianfeng Chemical Co.).

2.2. Synthesis and modification of ZSM-5 zeolites

The synthesis of ZSM-5 zeolite was according to the reported literature [37]. The gel molar composition was $300SiO_2$:$1Al_2O_3$:$90TPAOH$:$6000H_2O$:$450urea$. Detained synthesis procedure was carried out as follows: 104.2 g TEOS was added dropwise into 210.5 g TPAOH solution under stirring. After 12 h, 0.681 g Al(OPri)$_3$ was added into the mixture and stirred for 12h. After further addition of 45.0 g urea and stirred for 1 h, the resulting mixture was transferred into an autoclave. The crystallization was carried out at 180 °C for 48 h under tumbling 60 r/min. The as-made sample was centrifuged, washed with distilled water, dried at 120 °C overnight.

Typical post-synthetic modification treatment process with H_3PO_4 solution was as follows: 1.5 g as-made sample was added to 20.0 mL solution (1 mol/L) in a Teflon-lined stainless steel autoclave. After treatment at 90 °C for 12 h under tumbling 60 r/min, the slurry was filtered, washed with distilled water for three times until pH=7. All products were dried at 120 °C overnight and calcined at 550 °C for 8 h to remove the organic tem-

plate. In the case of Na_2H_2EDTA, the solution pH was adjusted to 1–2 by HCl and the final slurry was filtrated, followed by washing with large amount of hot water due to the low solubility of Na_2H_2EDTA. The ammonium exchange of calcined sample was carried out at 80 °C with NH_4NO_3 solution (1.0 mol/L) for three times to remove the possible residual sodium during the Na_2H_2EDTA treatment. The calcined precursor and samples modified by Na_2H_2EDTA and H_3PO_4 were named as ZSM-5, ZSM-5-E-*x*, ZSM-5-P-*x* respectively, where x represent the solution concentration.

2.3. Characterization

The powder XRD pattern was recorded on a PANalytical X'Pert PRO X-ray diffractometer with Cu-K_α radiation (λ = 0.15418 nm), operating at 40 kV and 40 mA. The chemical composition of solid samples was determined with a Philips-Magix-601 X-ray fluorescence (XRF) spectrometer. XPS measurements were performed using a Thermo ESCALAB 250Xi spectrometer with Al K_α radiation as the excitation source. The surface charge of the sample was calibrated by referencing to the Al 2*p* peak of Al_2O_3 at 74.7 eV. The crystal morphology was observed using a scanning electron microscopy (Hitachi SU8020). N_2 adsorption-desorption isotherms at –196 °C were determined on a Micromeritics ASAP2020. Prior to the measurement, samples were degassed at 350 °C under vacuum for 4 h. The total surface area was calculated based on the BET equation. The micropore volume and micropore surface area were evaluated using the t-plot method. ^{27}Al solid state NMR experiments were performed on a Varian Infinity plus 600 WB spectrometer with BBO MAS probe operating at magnetic field strength of 14.1 T. The resonance frequencies were 104.2 MHz and chemical shifts were referenced to 1.0 mol/L $Al(NO_3)_3$.The spinning rate of the samples at the magic angle was 4 kHz. Temperature-programmed desorption of ammonia (NH_3-TPD) was measured on a chemical adsorption instrument of Micrometric 2920. Each sample (40–60 mesh, 0.20 g) was loaded into a quartz U-shaped reactor and pretreated at 600 °C for 1 h in flowing He. After the pretreatment, the sample was cooled down to 100 °C and saturated with NH_3 gas. Then NH_3-TPD was carried out in a constant flow of He (20 mL/min) from 100 to 600 °C at a heating rate of 10 °C/min.

Fourier transform infrared (FT-IR) spectra after pyridine adsorption were obtained on a Bruker Tensor 27 instrument with a resolution of 4 cm^{-1}. Samples were pressed into a self-supporting wafer (R = 13 mm, 20 mg) and evacuated (10^{-2} Pa) in an IR cell at 723 K for 30 min prior to each measurement. Adsorption of pyridine was conducted at room temperature for 1 min to ensure saturated loading and then evacuation was carried out at 350 °C for 30 min and cooled down to room temperature prior to acquisition of IR spectra. The densities of Brønsted and Lewis acid sites were calculated from the IA values of the difference spectra at 1540 and 1450 cm^{-1}, respectively, using the extinction coefficients reported by Emeis [38].

2.4. Catalytic reaction

0.3 g calcined catalyst was pressed, sieved to 40–60 mesh and loaded in a fixed-bed quartz tubular reactor with inner diameter of 8 mm. Prior to the reaction, the catalyst was activated at 550 °C for 60 min, and then the temperature was adjusted to reaction temperature. Methanol was fed by passing the carrier gas (40.0 mL/min) through a saturator containing methanol at 35 °C, which gave a WHSV of 4.0 h^{-1}. Methanol conversion was performed under atmospheric pressure. The effluent products from reactor were kept at 200 °C and analyzed by an online Agilent 7890A GC equipped with a PONA capillary column (100 m × 0.25 mm × 0.5 μm) and a FID detector. The conversion and selectivity were calculated on CH_2 basis. Dimethyl ether (DME) was considered as reactant in the calculation. For the 1,3,5-triisopropylbenzene (TIPB) cracking reaction, similar condition was employed except that the reaction temperature was 360 °C.

2.5. Coke analysis

The coke percent of discharged catalysts was calculated by thermogravimetric analysis (TGA) and the loss between 300 to 700 °C was used to estimate coke content. Considering that the different amounts of methanol processed on each catalyst, the average coke deposition rate are defined as followed:

$$R_{coke} = 10C/((1–C/100) \times T \times M)$$

where: R_{coke} (mg/(g_{cat}·h)): the average coke deposition rate, C (%): the coke percent in discharged catalysts determined by TGA, T (h): reaction time, M (g): the catalyst amount.

The coke formation inside micropores (internal coke) was calculated from the decrease in the micropore volume determined by N_2 adsorption at –196 °C, assuming the coke density (d_{coke}) of 1.22 g/cm^3. The coke content deposited on the external surface was calculated by subtracting the internal coke content from the total coke content determined by TGA. The amounts of internal coke and external coke were calculated as follows [39–41]:

$$W_{internal\ coke} = (V_{micro,\ fresh} − V_{micro,\ after\ reaction} \times$$
$$(1 + W_{total\ coke})) \times d_{coke}$$
$$W_{external\ coke} = W_{total\ coke} − W_{internal\ coke}$$

where $W_{internal\ coke}$, $W_{external\ coke}$, and $W_{total\ coke}$ are the amounts (g_{coke}/g_{cat}) of internal, external, and total coke, respectively. $V_{micro,fresh}$ and $V_{micro,\ after\ reaction}$ are the micropore volumes (cm^3/g) of the catalysts before and after the reaction. d_{coke} is the coke density (1.22 g/cm^3).

3. Results and discussion

3.1. Characterization of ZSM-5 zeolites after post-synthetic treatment

The XRD patterns of ZSM-5 treated by Na_2H_2EDTA and H_3PO_4 solutions are shown in Fig. S1. It can be seen that ZSM-5-E-1 and ZSM-5-P-1 have a typical diffraction pattern of MFI topology, showing the high stability of as-made ZSM-5 to the post-synthetic treatment. The relative crystallinity calculated based on the intensity of the characteristic peaks at 7.8°, 8.8° and 22.4° are listed in Table S1. A decrease in relative

crystallinity was observed for ZSM-5-E-1. The SEM images of the samples are displayed in Fig. S2, showing a thin flakiness morphology with thickness of about 100 nm. No clear difference in the surface smoothness and morphology can be distinguished for the crystals before and after post-synthetic treatment. The N_2 adsorption-desorption isotherms and pore distributions of the samples are given in Fig. S3. The corresponding textural properties are listed in Table S1. It can be seen that the micropore surface area and micropore volume of the treated samples display a little increase, while the external surface area and mesopore volume slightly decrease. It is speculated that there may exist small amounts of amorphous materials on the shell region of the parent crystals, which was removed by the post-synthetic treatment.

Solid-state ^{27}Al MAS NMR spectra were measured to investigate the change of local atomic environments in the samples and are displayed in Fig. 1. One strong broad resonance centered around 56 ppm is observed for the calcined ZSM-5, which is attributed to tetrahedral Al species [42]. It implies that only framework Al atoms exist in the zeolite precursor. No obvious change can be found in the ^{27}Al MAS NMR spectra after post-synthetic treatment, indicating that the present strategy could effectively protect the framework Al atoms from dealumination by preventing access of the modifier into the crystal interior.

Table 1 lists the bulk and surface Si/Al ratios of the calcined samples. It can be seen that the bulk Si/Al ratio increases slightly for ZSM-5-E-1 and ZSM-5-P-1. On the other hand, the ZSM-5 precursor gives a surface Si/Al ratio of 60, which is obviously lower than the value of the bulk, implying an Al enrichment phenomenon on the crystal surface. The surface Si/Al ratios of the treated samples differ from each other; the value of ZSM-5-P-1 is close to the precursor, whereas a great increase is observed for ZSM-5-E-1. It is speculated that the as-made ZSM-5 has high resistance to the acid treatment, and Na_2H_2EDTA is more effective than acids for the dealumination of high-Si ZSM-5. Moreover, there is small amounts of P species left on ZSM-5-P-1 (0.17 wt%). The bulk and surface P/Al ratios of ZSM-5-P-1 are given in Table 1. An obviously higher surface P/Al ratio can be observed, implying that the P atoms are mainly located on the exterior of ZSM-5 crystals.

The acid properties of the samples were examined by NH_3-TPD and pyridine-adsorbed FT-IR. The results are summarized in Fig. 2 and Table 1. There exist two distinct desorption peaks centered around 180 and 380 °C in the NH_3-TPD curves (Fig. 2(a)), corresponding to weak and strong acid sites in the samples. In comparison with ZSM-5 precursor, ZSM-5-E-1 shows little change in the desorption temperature
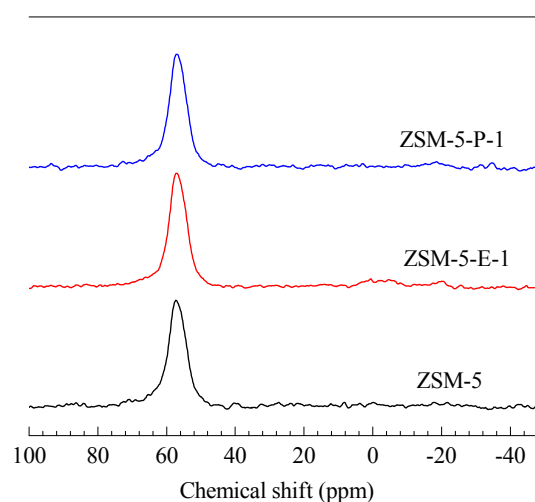

Fig. 1. ^{27}Al MAS NMR spectra of calcined samples.

and peak height. However, the intensity of high-temperature desorption peak of ZSM-5-P-1 drops slightly, indicating the decrease of strong acid sites. The acid density calculated based on the high-temperature desorption peak is listed in Table 1. The pyridine-adsorbed FT-IR spectra are displayed in Fig. 2(b). The peaks at 1540 and 1455 cm^{-1} are attributed to the vibrations associated with pyridine adsorption on Brønsted acid sites and Lewis acid sites, respectively [43]. The corresponding quantitative results are given in Table 1, which indicate that the treated samples possess a slightly higher Brønsted acid sites and lower Lewis acid sites than the precursor. The variations occur possibly due to the removal of the amorphous materials on the external surface and are consistent with the results in the part of textural characterization. The acidity characterization results together with the above paragraphs imply that the structural integrity in the crystal interior of ZSM-5 remains intact after the post-synthetic treatment.

TIPB cracking reaction was employed to investigate the external surface acidity of the samples (Fig. 3). ZSM-5-P-1 gives the lowest TIPB conversion among the samples. This is reasonable because the strong interactions between P and Al atoms on the P-rich surface can effectively decrease the number and strength of acid sites [44]. However, unexpectedly, ZSM-5-E-1 shows the highest catalytic activity. The TIPB conversions on ZSM-5-E-1 are more than twice as high as those of the precursor (the TIPB cracking experiment has been repeated over repeatedly prepared ZSM-5-E-1 and almost similar results are obtained). It seems contrary to the high

Table 1
The Si/Al ratio and acid properties of ZSM-5 before and after post-synthetic treatment.

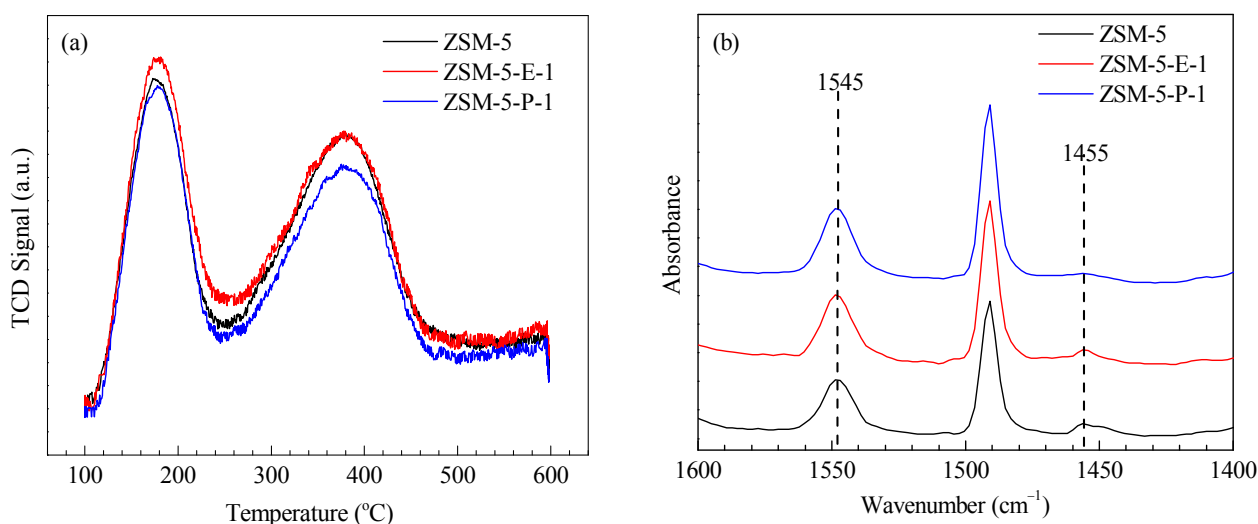| Catalyst	Bulk phase [a]		Surface phase [b]		Acid density by Py-IR (μmol/g)			Acid density by NH$_3$-TPD (μmol/g)
	Si/Al	P/Al	Si/Al	P/Al	B	L	B + L	
ZSM-5	124	–	60	–	112.2	15.5	127.6	112.6
ZSM-5-E-1	126	–	220	–	122.3	7.3	129.6	115.1
ZSM-5-P-1	130	0.44	78	2.17	119.6	5.8	125.4	104.3

[a] Determined by XRF. [b] Determined by XPS.

Fig. 2. NH$_3$-TPD curves (a) and pyridine-adsorbed FT-IR spectra (b) of ZSM-5 before and after post-synthetic treatment.

surface Si/Al ratio of ZSM-5-E-1 (Table 1). Possibly, silanol nests [45] are formed on the external surface of ZSM-5-E-1 crystals following the removal of framework Al atoms during the post-synthetic treatment. The silanol groups interacting through extended hydrogen bonding have moderate acidity and contribute to the enhanced TIPB cracking activity [47].

3.2. Catalytic performance in MTP reaction

Catalytic tests of methanol to olefins reaction over the samples were carried out at 480 °C with a methanol WHSV of 4.0 h^{-1}. The methanol conversion as a function of TOS is presented in Fig. 4. Both ZSM-5-E-1 and ZSM-5-P-1 show an improved catalytic lifetime as compared with the ZSM-5 precursor. Given that the crystal interiors of ZSM-5-E-1 and ZSM-5-P-1 are little influenced as revealed by the above characterizations, the improvement of catalytic lifetime should be closely related to the change of the surface properties.
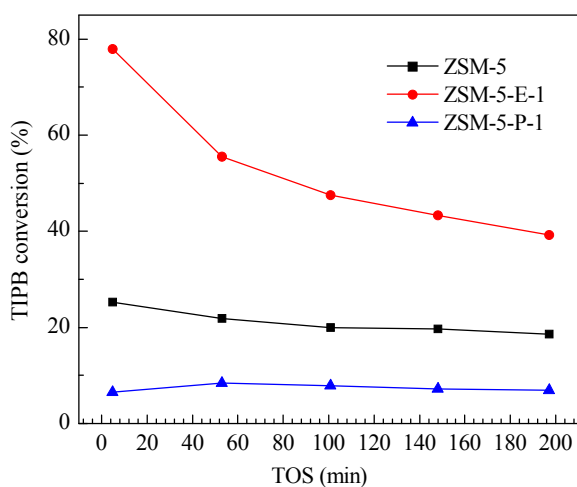

Fig. 3. TIPB conversion on ZSM-5 before and after post-synthetic treatment.

The coke content of discharged catalysts was determined by TG analysis (Fig. S4). The coke distributions in the micropores and on the external surface were estimated according to the results of N$_2$ physisorption and TG analysis. As shown in Fig. 4, the coke is mainly distributed on the external surface of ZSM-5 (at least 75% of the total coke content), which is consistent with the previous reports [9,39–41]. The treated samples possess more external coke than the precursor, indicating an increased tolerance to the external coke deposition. The corresponding coke deposition rate is shown in Fig. 4. ZSM-5-P-1 possesses lower external coke deposition rate, whereas ZSM-5-E-1 gives higher external coke deposition rate than the precursor. The variations of external coke deposition rate on the treated samples are consistent with the TIPB cracking results. On the other hand, both ZSM-5-E-1 and ZSM-5-P-1 give lower internal coke content and deposition rate than the precursor, which evidences an enhanced mass transfer in both samples (the micropores are more open after the treatment). It is inferred that the improved catalytic lifetime of ZSM-5-P-1 is due to a combination of the increased external tolerance to the external coke deposition and the depressed coking rate (reduced side reactions); but for ZSM-5-E-1, the increased tolerance to the external coke should be the major reason. Likely, the post-synthetic treatment removes the amorphous materials around the pore openings and helps improve the tolerance to the external coke deposition.

The products selectivities on the samples as a function of TOS are shown in Fig. 5. Moreover, detailed product distributions at TOS = 60 h are listed in Table 2. It can be seen that the ZSM-5 precursor gives propene as the most abundant product, followed by butene, C$_{5+}^N$ and ethene. The selectivities to ethene, propene and butene drop as the reaction proceeds, while those of C$_{5+}^N$ and aromatics increase. It is generally accepted that the reaction on ZSM-5 follows a dual-cycle mechanism: ethene mainly origins from the aromatics-based cycle, while propene and higher alkenes are formed to a considerable extent from the olefins-based cycle [46–48]. The
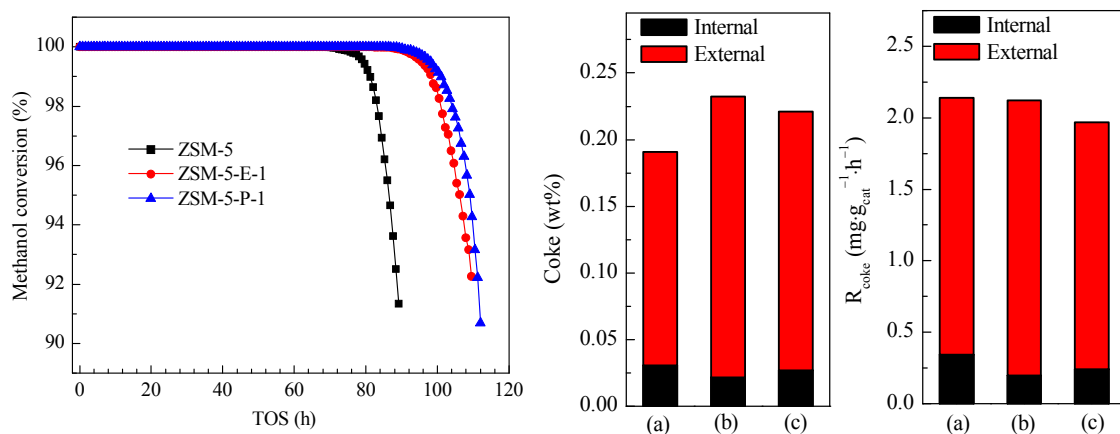
Fig. 4. The methanol conversion as a function of TOS, the coke content, coke distribution and coke deposition rate on the discharged ZSM-5 catalysts. (a) ZSM-5, (b) ZSM-5-E-1, (c) ZSM-5-P-1. Reaction conditions: 480 °C, methanol WHSV = 4.0 h^{-1}.
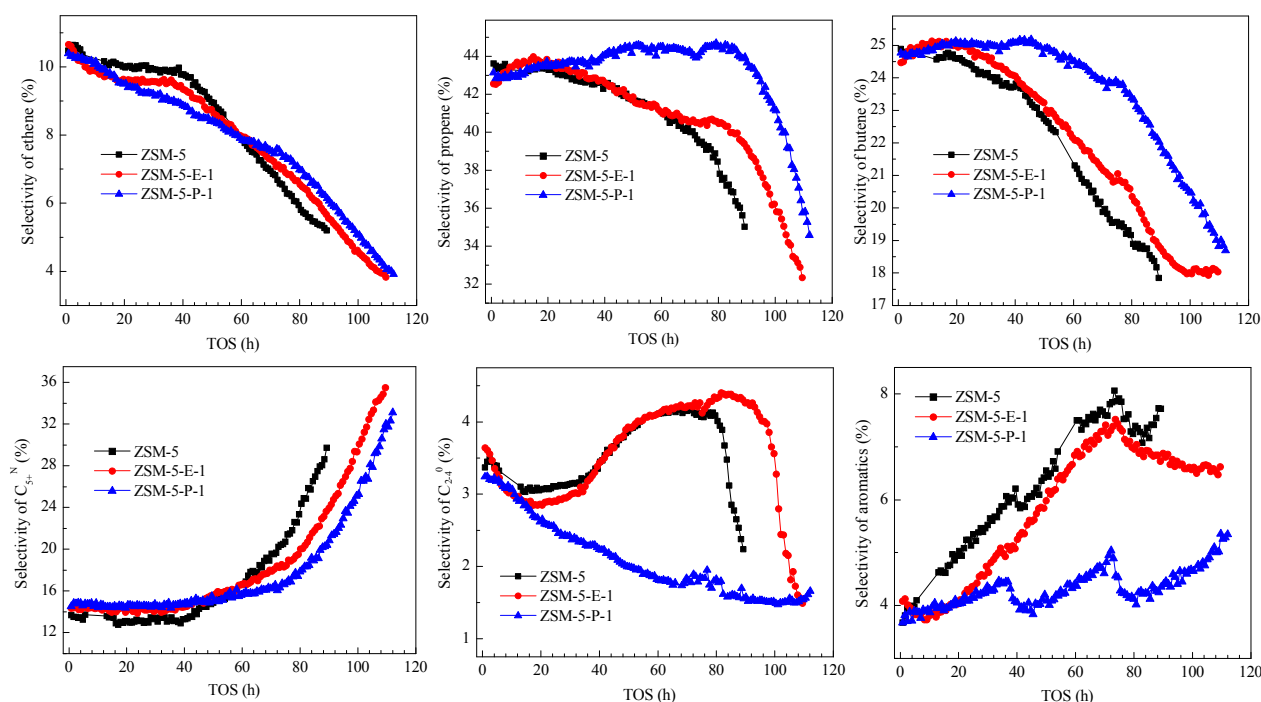
Fig. 5. Products selectivity as a function of TOS over ZSM-5 before and after post-synthetic treatment. Reaction conditions: 480 °C, methanol WHSV = 4.0 h^{-1}. The data fluctuation in the selectivity of aromatics over ZSM-5-P-1 is due to the interruption by adding methanol to the saturator.

depression of lower olefins as the increase of TOS implies a dropping activity of both cycles. The evolution trend of product selectivity on ZSM-5-E-1 resembles that on the ZSM-5 precursor, which suggests similar surface properties of the two samples despite their different surface Si/Al ratios. However, for ZSM-5-P-1, the selectivity of propene is maintained at high level until the deactivation; the selectivities of butene and C_{5+}^N are relatively stable at the first dozens of hours, while the ethene selectivity displays a continuous dropping trend. The higher propene selectivity on ZSM-5-P-1 should be attributed to the decreased external acid density, which abates the consecutive reaction of light olefins on the external surface and consists with its lower selectivities to C_{9+} aromatics (formed on the external acid sites) and alkanes (C_{2-4}^0). These results demonstrate that the reduction of external surface acid sites

can effectively improve both the catalytic lifetime and the stability of propene selectivity.

3.3. Influence of phosphoric acid concentration

Given the higher propene selectivity and longer lifetime observed on ZSM-5-P-1, the H_3PO_4 concentration in the post-synthetic treatment was further adjusted to optimize the catalytic performance. The product Si/Al ratios and P contents of the samples are summarized in Table 3. No regular change in the Si/Al ratio can be observed following the increase of H_3PO_4 concentration, and the samples have similar bulk and surface P contents. The insignificant effect of H_3PO_4 solution on the dealumination of high-Si as-made ZSM-5 is understandable, since high-Si zeolites are generally acknowledged to be

Table 2
Products distribution of the methanol conversion over ZSM-5 before and after post-synthetic treatment [a].

Sample	Lifetime (h)	Selectivity [b] (wt%)							
		CH_4	C_{2-4}^0	C_2H_4	C_3H_6	C_4H_8	C_{5+}^N	BTEX	A_{C9+}
ZSM-5	80	1.6	4.1	7.9	41.0	21.3	16.6	4.7	2.8
ZSM-5-E-1	98	1.3	4.1	7.9	41.0	22.1	16.7	4.5	2.4
ZSM-5-P-1	100	1.3	1.8	7.9	44.5	24.5	15.7	2.7	1.6
ZSM-5-P-3	118	1.0	1.9	8.7	44.1	25.4	14.6	2.9	1.3
ZSM-5-P-5	92	0.9	1.5	7.0	45.9	24.9	17.0	2.0	1.0

[a] Reaction conditions: 480 °C, WSHV = 4.0 h^{-1}. The lifetime is defined as methanol conversion of above 99%. [b] The data are collected at TOS = 60 h. C_{5+}^N non-aromatic products with carbon number > 4, BTEX: light aromatics with carbon number < 9, A_{C9+}: heavy aromatics with carbon number ≥ 9.

resistant to the acid solution. Indeed, we have carried out post-synthetic HCl treatment of the same precursor and almost unchanged Si/Al ratios are obtained (Table S2).

The TIPB conversions of the samples are also listed in Table 3. A gradual drop of the TIPB conversion can be observed following the increase of H_3PO_4 concentration, which implies the reduction of external acid density from ZSM-5-P-1 to ZSM-5-P-5. The TIPB cracking on pure Si silicalite-1 is also tested under the same conditions, which gives a conversion of 1.8% and confirms the existence of small amount of acid sites on the H_3PO_4-treated samples. The reduction in the external surface acid density as the increasing H_3PO_4 concentration may be caused by the slight degradation of surface structural integrity when ZSM-5 was treated under higher concentration acid solution.

Fig. 6 shows the methanol conversion results over the H_3PO_4-treated samples. The catalytic lifetime reaches a maximum of 118 h on ZSM-5-P-3 and reduces to 92 h on ZSM-5-P-5. The improvement in catalytic lifetime of ZSM-5-P-3 is apparently bigger than that of high-Si ZSM-5 with similar P loading (obtained by impregnation of HZSM-5 with H_3PO_4) in the previous report [49]. The coke content in the discharged catalysts was evaluated by TG analysis (Fig. S4) and the coke distributions in the crystal interior and on the external surface are also presented in Fig. 6. Clearly, ZSM-5-P-1 and ZSM-5-P-3 have similar external coke content, which is obviously higher than that on ZSM-5-P-5. The external coke deposition rate shows a reducing trend from ZSM-5-P-1 to ZSM-5-P-5, in accordance with the external acid density of the samples revealed by TIPB cracking. On the other hand, the internal coke content and deposition rate show a sequence of ZSM-5-P-3 < ZSM-5-P-5 < ZSM-5-P-1 < ZSM-5. The abnormal order between ZSM-5-P-3 and ZSM-5-P-5 suggests a reduced mass transfer in ZSM-5-P-5, which may be caused by the degradation of surface structural integrity of ZSM-5-P-5. This speculation is also

consistent with the lower external acid density (TIBP cracking ability) and lower tolerance to the external coke deposition on ZSM-5-P-5. It implies that suitable H_3PO_4 concentration in the post-synthetic treatment of as-made ZSM-5 is important to maximize the catalytic lifetime.

The product selectivities as a function of TOS over the samples are shown in Fig. S5. Detailed product distributions (TOS = 60 h) are presented in Table 2. Similar to ZSM-5-P-1, ZSM-5-P-3 and ZSM-5-P-5 display similar evolution trend of product selectivity as the reaction proceeds. The selectivities of propene, butene and C_{5+}^N are relatively stable at the first dozens of hours, while the selectivity to ethene drops gradually. From Table 2, the selectivities towards heavy aromatic and alkanes decrease gradually from ZSM-5-P-1 to ZSM-5-P-5, which implies the restrained side reactions and consist with their dropping external acid density. This also explains well the highest propene selectivity observed over ZSM-5-P-5 with the lowest external acid density.

4. Conclusions

In summary, we have presented a facile strategy to reduce the external surface acidity of high-silica ZSM-5 by utilizing the as-made zeolite as a precursor. The existence of OSDA in the as-made ZSM-5 crystals effectively blocks the channels and confines the modification on the crystal exterior without altering the internal acidity and integrity of the crystals. H_3PO_4

Table 3
The product compositions and TIPB conversion (TOS = 5 min) over ZSM-5 modified by H_3PO_4 solution with different concentrations.

Catalyst	Si/Al [a]	Si/Al [b]	P content (wt%)		TIPB conversion (%)
			Bulk [a]	Surface [b]	
ZSM-5-P-1	130	78	0.17	1.38	6.5
ZSM-5-P-3	132	55	0.12	1.21	5.7
ZSM-5-P-5	128	79	0.13	1.30	4.5
Silicalite-1	–	–	–	–	1.8

[a] Determined by XRF. [b] Determined by XPS.
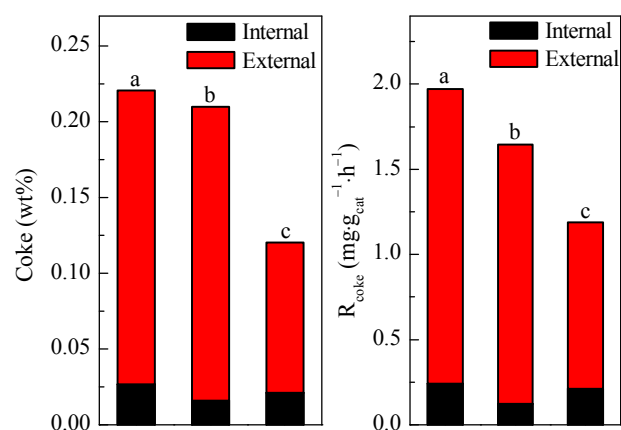
Fig. 6. The methanol conversion as a function of TOS, the coke content, coke distribution and coke deposition rate over ZSM-5 before and after the H_3PO_4 Treatment. (a) ZSM-5-P-1, (b) ZSM-5-P-3, (c) ZSM-5-P-5. Reaction conditions: 480 °C, methanol WHSV=4.0 h^{-1}.

treatment cannot remove surface Al atoms, but the small amount of P left on the external surface effectively decreases the acid density. Na_2H_2EDTA treatment selectively removes the surface Al atoms. However, new acid sites (likely silanol nests) are generated on the external surface after Na_2H_2EDTA treatment. Both Na_2H_2EDTA and H_3PO_4 treatments can prolong the catalytic lifetime of ZSM-5 in the MTP reaction. The reduced external surface acid density on the H_3PO_4-treated ZSM-5 has a lower external coke deposition rate (reduced side reactions), which helps the sample show higher propene selectivity. Under the optimized H_3PO_4 concentration, the treated ZSM-5 extends the catalytic lifetime from 80 h of the precursor to 118 h.

References

[1] H. Koempel, W. Liebner, *Stud. Surf. Sci. Catal.*, **2007**, 167, 261–267.

[2] X. Zhao, L. Wang, J. Li, S. Xu, W. Zhang, Y. Wei, X. Guo, P. Tian, Z. Liu, *Catal. Sci. Technol.*, **2017**, 7, 5882–5892.

[3] M. Khanmohammadi, S. Amani, A. B. Garmarudi, A. Niaei, *Chin. J. Catal.*, **2016**, 37, 325–339.

[4] J. Wang, J. Li, S. Xu, Y. Zhi, Y. Wei, Y. He, J. Chen, M. Zhang, Q. Wang, W. Zhang, X. Wu, X. Guo, Z. Liu, *Chin. J. Catal.*, **2015**, 36, 1392–1402.

[5] D. M. Bibby, R. F. Howe, G. D. McLellan, *Appl. Catal. A*, **1992**, 93, 1–34.

[6] S. Mueller, Y. Liu, M. Vishnuvarthan, X. Sun, A. C. van Veen, G. L. Haller, M. Sanchez-Sanchez, J. A. Lercher, *J. Catal.*, **2015**, 325, 48–59.

[7] M. Guisnet, P. Magnoux, *Appl. Catal. A*, **2001**, 212, 83–96.

[8] Q. Guo, D. Mao, Y. Lao, G. Lu, *Chin. J. Catal.*, **2009**, 30, 1248–1254.

[9] M. Guisnet, L. Costa, F. R. Ribeiro, *J. Mol. Catal. A*, **2009**, 305, 69–83.

[10] C. S. Chen Hsia, S. E. Schramm, *Microporous Mater.*, **1996**, 7, 125–132.

[11] J. Nunan, J. Cronin, J. Cunningham, *J. Catal.*, **1984**, 87, 77–85.

[12] L. D. Rollmann, *Stud. Surf. Sci. Catal.*, **1991**, 68, 791–797.

[13] L.Y. Fang, S. B. Liu, I. Wang, *J. Catal.*, **1999**, 185, 33–42.

[14] T. Hibino, M. Niwa, Y. Murakami, *J. Catal.*, **1991**, 128, 551–558.

[15] T. Hibino, M. Niwa, Y. Murakami, *Zeolites*, **1993**, 13, 518–523.

[16] Y. H. Yue, Y. Tang, Y. Liu, Z. Gao, *Ind. Eng. Chem. Res.*, **1996**, 35, 430–433.

[17] H. Zhang, M. Luo, R. Xiao, S. Shao, B. Jin, G. Xiao, M. Zhao, J. Liang, *Bioresour. Technol.*, **2014**, 155, 57–62.

[18] Z. R. Zhu, Q. L. Chen, Z. K. Xie, W. M. Yang, D. J. Kong, C. Li, *J. Mol. Catal. A*, **2006**, 248, 152–158.

[19] Y. Wang, L. Xu, Z. Yu, X. Zhang, Z. Liu, *Chin. J. Catal.*, **2008**, 29, 1237–1241.

[20] Y. Bouizi, L. Rouleau, V. P. Valtchev, *Chem. Mater.*, **2006**, 18, 4959–4966.

[21] D. Van Vu, M. Miyamoto, N. Nishiyama, Y. Egashira, K. Ueyama, *J. Catal.*, **2006**, 243, 389–394.

[22] C. S. Lee, T. J. Park, W. Y. Lee, *Appl. Catal. A*, **1993**, 96, 151–161.

[23] K. Miyake, Y. Hirota, K. Ono, Y. Uchida, S. Tanaka, N. Nishiyama, *J. Catal.*, **2016**, 342, 63–66.

[24] N. Liu, X. Zhu, S. Hua, D. Guo, H. Yue, B. Xue, Y. Li, *Catal. Commun.*, **2016**, 77, 60–64.

[25] J. Ding, T. Xue, H. Wu, M. He, *Chin. J. Catal.*, **2017**, 38, 48–57.

[26] Y. Song, L. l. Zhang, G. D. Li, Y. S. Shang, X. M. Zhao, T. Ma, L. M. Zhang, Y. L. Zhai, Y. J. Gong, J. Xu, F. Deng, *Fuel Process. Technol.*, **2017**, 168, 105–115.

[27] S. Zhang, Y. Gong, L. Zhang, Y. Liu, T. Dou, J. Xu, F. Deng, *Fuel Process. Technol.*, **2015**, 129, 130–138.

[28] J. L. Hodala, A. B. Halgeri, G. V. Shanbhag, *Appl. Catal. A*, **2014**, 484,

---

Graphical Abstract

External surface modification of as-made ZSM-5 and their catalytic performance in the methanol to propylene reaction

Xuebin Zhao, Yang Hong, Linying Wang, Dong Fan, Nana Yan, Xiaona Liu, Peng Tian *, Xinwen Guo *, Zhongmin Liu *
Dalian University of Technology; Dalian Institute of Chemical Physics, Chinese Academy of Sciences; University of Chinese Academy of Sciences
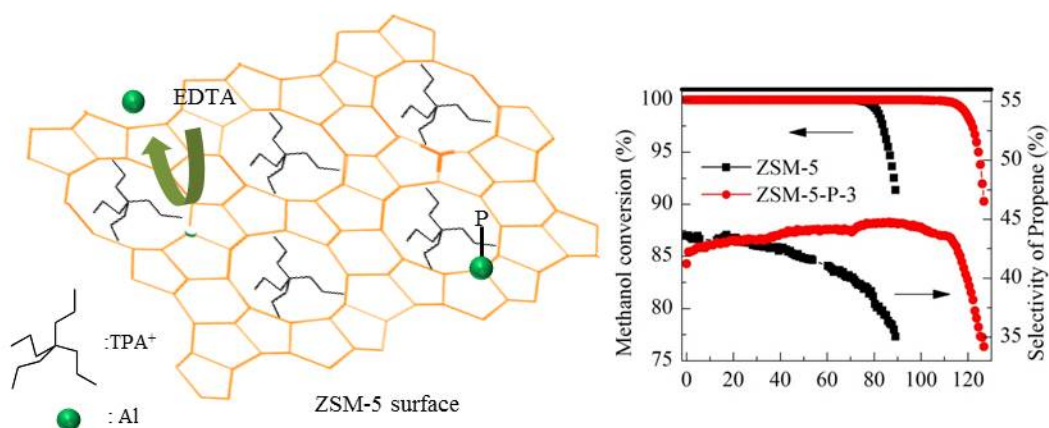
Post-synthetic treatment of as-made ZSM-5 with Na_2H_2EDTA or H_3PO_4 solution can prolong the MTP reaction lifetime of ZSM-5. The H_3PO_4 modification can further enhance the propene selectivity due to the depressed external coke deposition rate (reduced side reactions).

8–16.

[29] P. Losch, M. Boltz, C. Bernardon, B. Louis, A. Palcic, V. Valtchev, *Appl. Catal. A*, **2016**, 509, 30–37.

[30] Y. Zhao, J. Liu, G. Xiong, H. Guo, *Chin. J. Catal.*, **2017**, 38, 138–145.

[31] S. M. Abubakar, D. M. Marcus, J. C. Lee, J. O. Ehresmann, C. Y. Chen, P. W. Kletnieks, D. R. Guenther, M. J. Hayman, M. Pavlova, J. B. Nicholas, J. F. Haw, *Langmuir*, **2006**, 22, 4846–4852.

[32] N. Xue, R. Olindo, J. A. Lercher, *J. Phys. Chem. C*, **2010**, 114, 15763–15770.

[33] l. lei, [MS Dissertation], Dalian University of Technology, Dalian, **2014**, 31–42.

[34] N. Li, Y. Y. Zhang, L. Chen, C. T. Au, S. F. Yin, *Microporous Mesoporous Mater.*, **2016**, 227, 76–80.

[35] S. Inagaki, S. Shinoda, Y. Kaneko, K. Takechi, R. Komatsu, Y. Tsuboi, H. Yamazaki, J. N. Kondo, Y. Kubota, *ACS Catal.*, **2013**, 3, 74–78.

[36] G. T. Kerr, *J. Phys. Chem.*, **1968**, 72, 2594–2596.

[37] Y. Liu, X. Zhou, X. Pang, Y. Jin, X. Meng, X. Zheng, X. Gao, F. S. Xiao, *ChemCatChem*, **2013**, 5, 1517–1523.

[38] C. A. Emeis, *J. Catal.*, **1993**, 141, 347–354.

[39] K. Lee, S. Lee, Y. Jun, M. Choi, *J. Catal.*, **2017**, 347, 222–230.

[40] M. Choi, K. Na, J. Kim, Y. Sakamoto, O. Terasaki, R. Ryoo, *Nature*, **2009**, 461, 246–250.

[41] D. M. Bibby, N. B. Milestone, J. E. Patterson, L. P. Aldridge, *J. Catal.*, **1986**, 97, 493–502.

[42] E. Lippmaa, A. Samoson, M. Magi, *J. Am. Chem. Soc.*, **1986**, 108, 1730–1735.

[43] J. Li, S. Liu, H. Zhang, E. Lu, P. Ren, J. Ren, *Chin. J. Catal.*, **2016**, 37, 308–315.

[44] H. E. van der Bij, B. M. Weckhuysen, *Chem. Soc. Rev.*, **2015**, 44, 7406–7428.

[45] H. Munakata, T. R. Koyama, T. Yashima, N. Asakawa, T. O-Nuki, K. Motokura, A. Miyaji, T. Baba, *J. Phys. Chem. C*, **2012**, 116, 14551–14560.

[46] M. Bjorgen, S. Svelle, F. Joensen, J. Nerlov, S. Kolboe, F. Bonino, L. Palumbo, S. Bordiga, U. Olsbye, *J. Catal.*, **2007**, 249, 195–207.

[47] P. Tian, Y. Wei, M. Ye, Z. Liu, *ACS Catal.*, **2015**, 5, 1922–1938.

[48] D. Lesthaeghe, A. Horre, M. Waroquier, G. B. Marin, V. Van Speybroeck, *Chem. Eur. J.*, **2009**, 15, 10803–10808.

[49] J. Liu, C. Zhang, Z. Shen, W. Hua, Y. Tang, W. Shen, Y. Yue, H. Xu, *Catal. Commun.*, **2009**, 10, 1506–1509.

高硅ZSM-5原粉的外表面改性及其在甲醇制丙烯反应中的应用

赵学斌[a,b,c], 洪　杨[b,c], 王林英[b], 樊　栋[b], 闫娜娜[b,c], 刘晓娜[b,c], 田　鹏[b,#], 郭新闻[a,*], 刘中民[b,$]

[a]大连理工大学化工学院, 宾州州立大学-大连理工大学联合能源研究中心, 精细化工国家重点实验室, 辽宁大连116024

[b]中国科学院大连化学物理研究所, 甲醇制烯烃国家工程实验室, 国家能源低碳催化与工程研发中心,

洁净能源国家实验室, 能源材料化学协同创新中心, 辽宁大连116023

[c]中国科学院大学, 北京100049

摘要: 使用来源广泛的甲醇为原料制取丙烯, 是对石油路线生产丙烯的重要补充. 尽管以ZSM-5分子筛为催化剂的固定床甲醇制丙烯(MTP)技术已经实现了工业应用, 但进一步提高催化剂的寿命和丙烯的选择性一直是学术界和工业界的研究热点. MTP过程作为典型的酸催化反应, 积碳是催化剂失活的主要原因, 由于ZSM-5分子筛十元环孔道的空间限制作用, 积碳主要分布在外表面. 因此, 消除外表面的酸性位点对延长催化剂的寿命至关重要, 但修饰外表面酸性位点的同时往往会改变样品的其他性质, 如孔径、整体酸量等. 本文分别使用Na_2H_2EDTA和H_3PO_4处理高硅ZSM-5分子筛原粉(微孔内含有机模板剂)来选择性地减小或消除外表面的酸密度, 而不影响分子筛内部的性质, 并考察了处理后样品的MTP性能. 使用N_2物理吸附、SEM和^{27}Al MAS NMR表征样品的织构性质、形貌和Al原子的化学环境, XPS和三异丙苯裂解实验表征外表面的硅铝比和酸密度. 表征结果表明, Na_2H_2EDTA处理虽然可以选择性的脱除表面Al原子, 但会在外表面产生新的酸点(可能是硅巢). H_3PO_4处理虽然不能脱除表面的Al原子, 但外表面残留的P物种能够有效的减小酸密度. MTP评价结果表明, H_3PO_4处理能够有效的延长催化剂的寿命和维持丙烯的选择性, 这是因为H_3PO_4处理既提高了外表面的容碳能力, 也抑制了积碳沉积的速率. Na_2H_2EDTA处理仅能增加外表面的容碳能力, 所以其只能延长催化寿命. 通过进一步优化H_3PO_4后处理的条件, 处理后的ZSM-5样品的催化寿命可以延长至前体的1.5倍, 同时, 丙烯的选择性也略有提高, 并且在失活前维持增加的趋势.

关键词: 甲醇制丙烯; ZSM-5分子筛; 改性; 磷酸; 乙二胺四乙酸

For Author Index:

ZHAO Xuebin, HONG Yang, WANG Linying, FAN Dong, YAN Nana, LIU Xiaona, TIAN Peng, GUO Xinwen, LIU Zhongmin

Supporting Information for

External surface modification of as-made ZSM-5 and their catalytic performance in the methanol to propylene reaction

Xuebin Zhao [a,b,c], Yang Hong [b,c], Linying Wang [b], Dong Fan [b], Nana Yan [b,c], Xiaona Liu [b,c], Peng Tian [b,#], Xinwen Guo [a,*], Zhongmin Liu [b,$]

[a] *State Key Laboratory of Fine Chemicals, PSU-DUT Joint Center for Energy Research, School of Chemical Engineering, Dalian University of Technology, Dalian 116024, Liaoning, China*

[b] *National Engineering Laboratory for Methanol to Olefins, State Energy Low Carbon Catalysis and Engineering R&D Center, Dalian National Laboratory for Clean Energy, Collaborative Innovation Center of Chemistry for Energy Materials (iChEM), Dalian Institute of Chemical Physics, Chinese Academy of Sciences, Dalian 116023, Liaoning, China*

[c] *University of Chinese Academy of Sciences, Beijing 100049, China*

* Corresponding author. Tel: +86-411-84986133; Fax: +86-411-84986134; E-mail: guoxw@dlut.edu.cn
* Corresponding author. Tel: +86-411-84379218; Fax: +86-411-84379289; E-mail: tianpeng@dicp.ac.cn
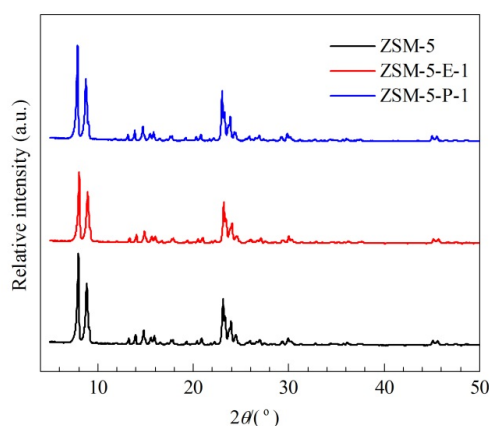$ Corresponding author. Tel: +86-411-84379998; Fax: +86-411-84379289; E-mail: liuzm@dicp.ac.cn

Fig. S1. XRD patterns of as-made ZSM-5 before and after post-synthetic treatment.

Table S1
Relative crystallinity and texture properties of ZSM-5 before and after post-synthetic treatment.

| Catalyst	R [a]	Surface area [b] (m²/g)			Pore volume [c] (cm³/g)	
		S_{BET}	S_{micro}	S_{ext}	V_{micro}	V_{ext}
ZSM-5	100	377	318	60	0.151	0.078
ZSM-5-E-1	81.2	392	349	43	0.164	0.058
ZSM-5-P-1	103.8	380	331	49	0.156	0.066

[a] Relative crystallinity calculated based on the intensity of the characteristic peaks at 7.8°, 8.8° and 22.4°; [b] S_{BET}: BET surface area, S_{micro}: t-plot microporous surface area, $S_{ext} = S_{BET} - S_{micro}$; [c] V_{micro}: t-plot microporous volume, $V_{ext} = V_{total} - V_{micro}$ (V_{total} is evaluated at $P/P_0 = 0.99$).

Fig. S2. SEM images of ZSM-5 zeolites before and after post-synthetic treatment.
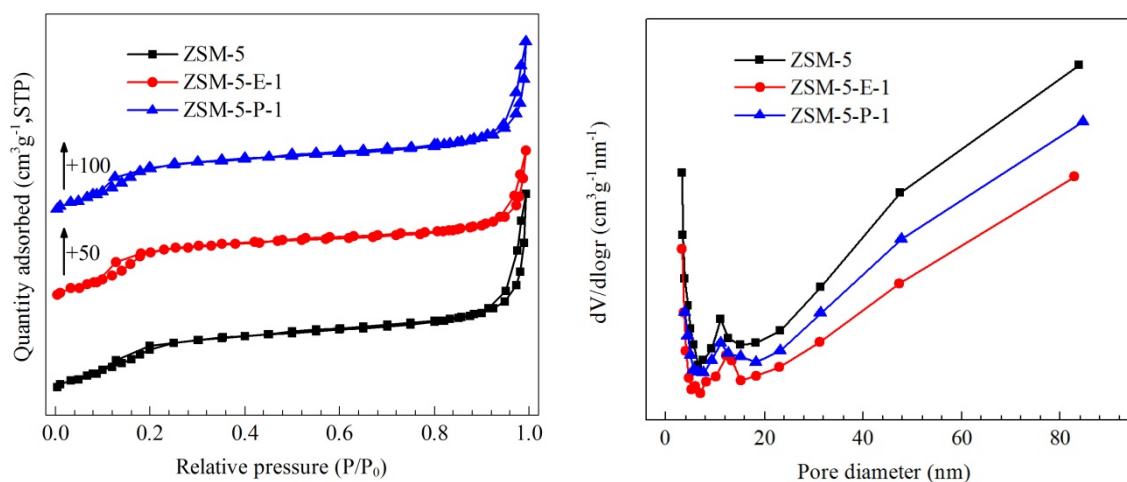
Fig. S3. N$_2$ adsorption-desorption isotherms and pore size distribution curve calculated from the adsorption branch of ZSM-5 before and after post-synthetic treatment.
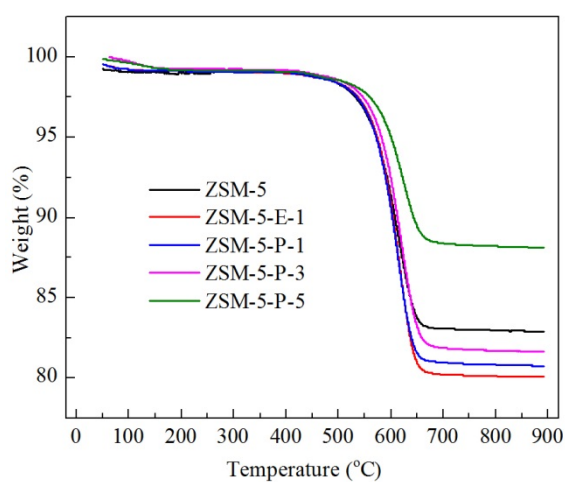
Fig. S4. TG curves of discharged ZSM-5 catalysts after the methanol conversion reaction.

Table S2

The Si/Al ratio of ZSM-5 before and after post-synthetic HCl treatment. [a]

Sample	Si/Al$_{Bulk}$ [b]	Si/Al$_{Surface}$ [c]
ZSM-5	124	60
ZSM-5-H-1	124	44

[a] Treatment condition for ZSM-5-H-1: 1 mol/L HCl solution, 90 °C, 12 h.

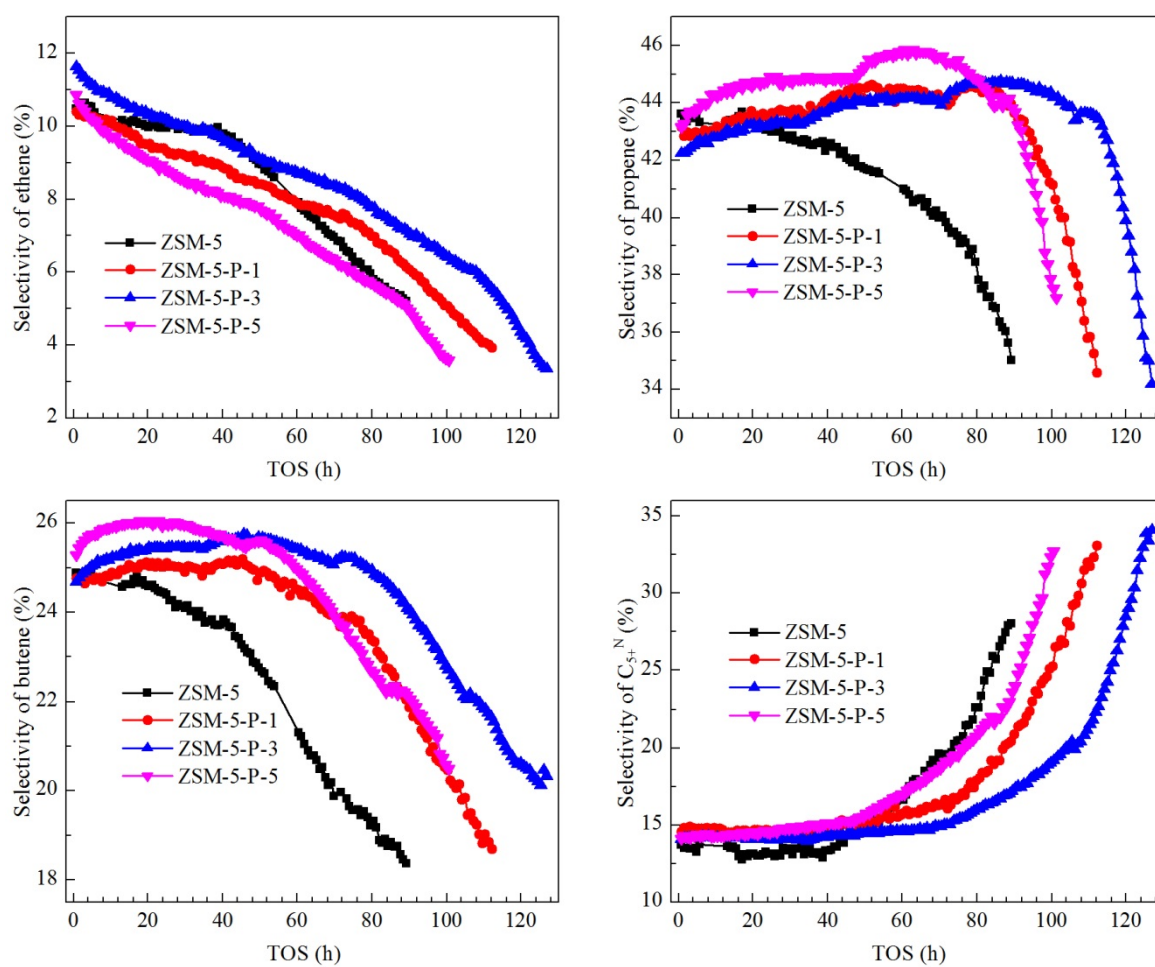[b] Determined by XRF.

[c] Determined by XPS.

Fig. S5. Product selectivities as a function of TOS over ZSM-5 zeolites modified by H_3PO_4 solution with different concentration.